Heterojunction wavelength-tailorable far-infrared photodetectors with response out to 70 μm

A. G. U. Perera,[a)] S. G. Matsik, and B. Yaldiz
Department of Physics and Astronomy, Georgia State University, Atlanta, Georgia 30303

H. C. Liu, A. Shen, M. Gao, Z. R. Wasilewski, and M. Buchanan
Institute for Microstructural Studies, NRC-Canada, Ottawa, Ontario, Canada

(Received 24 October 2000; accepted for publication 12 February 2001)

Results are presented on the performance of a heterojunction interfacial workfunction internal photoemission (HEIWIP) wavelength-tailorable detector. The detection mechanism is based on free-carrier absorption in the heavily doped emitter regions and internal emission across a workfunction barrier caused by the band gap offset at the heterojunction. The HEIWIP detectors have the high responsivity of free-carrier absorption detectors and the low dark current of quantum well infrared photodector type detectors. For a 70 ± 2 cutoff wavelength detector, a responsivity of 11 A/W and a $D^* = 1\times10^{13}\,\mathrm{cm}\sqrt{\mathrm{Hz}}/\mathrm{W}$ with a photocurrent efficiency of 24% was observed at 20 μm. From the 300 K background photocurrent, the background limited performance (BLIP) temperature for this HEIWIP detector was estimated to be 15 K. This HEIWIP detector provides an exciting approach to far-infrared detection.
[DOI: 10.1063/1.1361283]

Far-infrared (FIR) detectors are of interest for various astronomy applications such as the Stratospheric Observatory for Infrared Astronomy (SOFIA) program and Explorer missions. Stressed Ge (Ref. 1) and blocked impurity band[2] detectors have been studied for almost 20 years as FIR detectors. Due to the material constraints in Ge, homojunction interfacial workfunction internal photoemission infrared photodetectors (HIWIPs) using Si and GaAs have been studied as an alternative detector structure.[3] HIWIP detectors consist of successive highly doped emitter layers and undoped barrier layers. Detection takes place by free-carrier absorption in the emitter layers followed by the internal photoemission of photoexcited carriers across the barrier and collection.[3] The cutoff wavelength (λ_c) is determined by the workfunction Δ (the difference between the barrier conduction band and the 3D Fermi level in the emitters) at the interface. By adjusting the device parameters, mainly the doping concentration in the emitter region, λ_c can be tailored to the desired range. Once the device is designed λ_c can also be tailored using the applied electric field.

HIWIP structures have shown high responsivity and good detectivity in this range, but have high dark current associated with higher doping required for longer wavelength operation, and lower quantum efficiencies. The workfunction in HIWIPs is due to the band gap narrowing effect in the highly doped emitter regions. High density (HD) theory, where only the dopant type (n or p) is considered but not the specific impurities, has been used to calculate the workfunction associated with doping concentration.[4] As the concentration is increased, the doping accuracy required to achieve a consistent workfunction for detection at wavelengths beyond 200 μm becomes more stringent. In addition, the most common p-dopant, beryllium, diffuses spontaneously at the concentrations required for response beyond 200 μm. The diffusion problems may be eliminated by using carbon as the dopant. However, even with the reduced diffusion, the high precision in doping density and the uncertainty associated with the band gap narrowing still place potential limits on the use of HIWIPs.

In this letter results are presented on heterojunction interfacial workfunction internal photoemission (HEIWIP) far-infrared detectors where the workfunction is primarily due to an AlGaAs layer next to a doped GaAs (emitter) layer. The emitters are doped to a sufficiently high level so that the carriers form a three-dimensional (3D) distribution in the emitters and detection is by free-carrier absorption just as in the case of HIWIPs. However this will still be very much below the concentrations needed for HIWIP detectors. The barriers have a low Al fraction so that the workfunction[4] will be small, allowing operation at FIR wavelengths. By adjusting the Al fraction (and to a lesser extent the emitter doping density) λ_c can be tailored to any desired wavelength. The doping in the emitters of the GaAs/AlGaAs structures should be kept low ($\leq 10^{19}\,\mathrm{cm}^{-3}$) to reduce the dark current to levels comparable to or lower than those of quantum well infrared photodetectors (QWIPs), while the use of free-carrier absorption in the emitter regions rather than the intersubband transition used in QWIPs will give the high responsivity observed in HIWIPs. The optimum doping of the emitter regions will have to be determined by balancing the dark current and absorption quantum efficiency in the emitter regions. Thus HEIWIPs can combine the best properties of the QWIP and HIWIP detectors leading to improved operation.

The device structure [confirmed using secondary ion mass spectroscopy (SIMS)] consists of 20 periods of 158 Å GaAs emitters and 800 Å $Al_{0.02}Ga_{0.98}As$ barriers. The emitters were doped with Be to $3\times10^{18}\,\mathrm{cm}^{-3}$. The top and bottom contacts were Be doped to $1\times10^{19}\,\mathrm{cm}^{-3}$ with thicknesses of 0.4 and 0.8 μm, respectively. The devices were fabricated by etching $400\times400\,\mu\mathrm{m}^2$ mesas using standard wet etching techniques and then evaporating Ti/Pt/Au ohmic

[a)]Electronic mail: uperera@gsu.edu

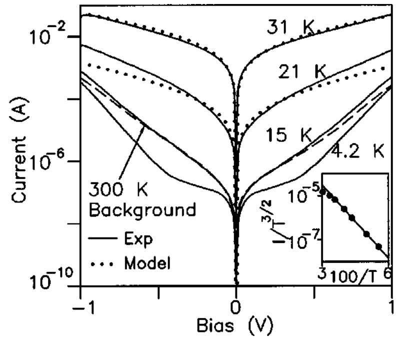

FIG. 1. Dark current at various temperatures for the HEIWIP detector. The dark current at 10 K is almost the same as that for 4.2 K. Also shown is the 300 K background current (dashed line) indicating BLIP operation at 15 K. A fit to the thermionic dark current based on a 3D drift model (Ref. 7) is shown for 21 and 31 K. Activation energies of 19.5 and 19 meV were used in modeling the forward and reverse directions, respectively. The inset shows the Arrhenius plot used to obtain an activation energy of 19 ± 1 meV.

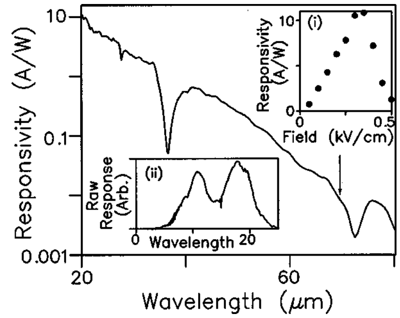

FIG. 3. Responsivity spectra for the HEIWIP detector at 0.7 V bias obtained at 4.2 K. The cutoff wavelength indicated by the vertical arrow where the responsivity reaches the noise level was 70 ± 2 μm. The sharp decrease between 35 and 40 μm is due to reflection from the front face of the detector. The responsivity remained the same to 8 K and then decreased at higher temperatures. Inset (i) shows the responsivity at 20 μm. Inset (ii) shows that the raw spectrum at shorter wavelengths with a zero response at 25 μm due to a beam splitter minimum.

contacts onto the top and bottom contact layers. A 260 $\times 260$ μm^2 window was opened, through the top contact to provide front illumination to the device.

Figure 1 shows the dark current for the HEIWIP detector at various temperatures. Also shown is the 300 K background photocurrent at 4.2 K coinciding with the 15 K dark current giving a BLIP temperature of 15 K for the detector. Above 10 K the current is primarily thermionic and an Arrhenius plot for 10 mV bias (inset in Fig. 1) gives an activation energy (workfunction) of 19 ± 1 meV corresponding to a λ_c of 65 ± 5 μm. Based on the measured device parameters using SIMS data the estimated work function Δ [the energy difference between the Fermi level and the barrier seen in the band diagram shown in Fig. 2] including both the band gap narrowing in the emitters and the AlGaAs band gap offset was ~ 21 meV giving an expected λ_c of 61 μm. The discrepancy between the predicted work function and the Arrhenius plot result may be due to small variations in the Al fraction and/or in the band gap narrowing in the emitters. Below 10 K the dark current was primarily due to tunneling and did not change with temperature, having almost identical dark current curves at 4.2 and 10 K. The dark current at a given electric field is ~ 200 times less than for a HIWIP detector[3] with a similar workfunction, indicating a dramatic improvement in dark current.

The responsivity of the detector was measured using a Perkin-Elmer system 2000 Fourier transform infrared (FTIR) spectrometer with a Si composite bolometer as a reference detector. The results obtained for the HEIWIP at 0.7 V bias for 4.2 K are shown in Fig. 3. The response increases with increasing bias until ~ 0.7 V [see inset (i) of Fig. 3] and starts decreasing as the bias is increased further. The same type of behavior has been observed for HIWIP detectors and is believed to be related to impact ionization in the barrier region. This leads to increased dark current and reduced responsivity above a critical field.[4] A strong response is observed for wavelengths shorter than 50 μm with λ_c (zero response) of 70 ± 2 μm as indicated by the arrow in Fig. 3, consistent with the Arrhenius plot results. The responsivity was 0.5 A/W at 40 μm, increasing to 2.8 and 11 A/W at 30 and 20 μm, respectively, for 0.7 V bias. This is slightly higher than the highest responsivity obtained from HIWIP detectors[3] and a factor of 6 improvement on the 0.45 A/W obtained from QWIPs at 30 μm.[5] This confirms the HEIWIP detectors will show the high responsivity seen in HIWIPs rather than the lower responsivity seen in QWIPs. Internal photoemission is more efficient at lower wavelengths,[4] with the free-carrier absorption expected to be proportional to λ^2 causing the responsivity to increase as wavelength increases. At long wavelengths the free-carrier absorption is independent of the wavelength, and the responsivity decreases with increasing wavelength due to the decreasing internal photoemission. The transition between the short and long wavelength behavior of the absorption is expected to be in the range of 8–12 μm.[6] The shape of the responsivity spectrum (see Fig. 3) corresponds to the expected results. The raw response [see inset (ii) of Fig. 3] starts increasing with the wavelength from about 3.5 μm and starts decreasing beyond 18 μm, with a peak near 10 μm. Spectra measured for different detector temperatures showed constant responsivity up to 11 K and decreased at 16 K which is consistent with the estimated background limited performance (BLIP) from the dark and 300 K background currents.

For a bias of 0.7 V the noise at frequencies above 400 Hz was $S_I \sim 9\times 10^{-29}$ A^2/Hz, which is much lower than the HIWIP values, indicating an improvement in device quality. Based on this noise value the detectivity was $\sim 1 \times 10^{13}$ cm$\sqrt{\mathrm{Hz}}$/W which is a significant improvement over 5.9×10^{10} cm$\sqrt{\mathrm{Hz}}$/W obtained for a high performance HIWIP detector.[3] The noise equivalent power (NEP) was 3.0×10^{-15} W/$\sqrt{\mathrm{Hz}}$, again about a factor of 100 better than that for the HIWIP. The photocurrent efficiency for the detector was determined by dividing the photocurrent by the number of incident photons, resulting in an efficiency of 24% for the

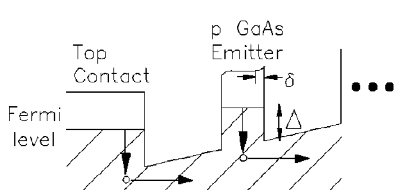

FIG. 2. A partial band diagram for the HEIWIP detector with the workfunction Δ and the effective width of the zero field region δ indicated.

HEIWIP detector at 20 μm, a 100% improvement on the best HIWIP result reported to date of 12.5% (Ref. 3) for a sample with the same number of layers and similar thicknesses.

The increased D^* compared to that of QWIPs can be understood by looking at the dark current and the absorption quantum efficiency. For the HEIWIP structure the dark current can be predicted by a 3D carrier drift model[7] given by

$$j_H = e\frac{\mu E}{[1+(\mu E/v_{\rm sat})^2]^{1/2}} 2(m_H k_B T/2\pi\hbar^2)^{3/2} \times \exp(-(\Delta - \alpha_H E)/k_B T), \quad (1)$$

where μ is the mobility, E is the electric field, $v_{\rm sat}$ is the saturation drift velocity, m_H is the carrier effective mass, Δ is the activation energy, and α_H is a fitting parameter that determines the effective barrier lowering. Model results for the detector at 21 and 31 K using $\mu = 80\,{\rm cm}^2/{\rm V\,s}^{-1}$, $\alpha_H = 80$ Å, and Δ of 19.5 meV for forward bias and 19.0 meV for reverse bias are shown in Fig. 1 and indicate a reasonable fit. The small difference in barrier height for different polarities can be due to possible variations in the Al fraction at the two ends. Although the same result should be valid for HIWIPs, the experimentally observed dark current is ~ two orders of magnitude larger than that for HEIWIPs. This improvement is probably related to differences in the barrier lowering parameter. This parameter reflects different causes of barrier lowering, such as space charge, the image force effect, and interface thickness, related to the transition from highly doped emitters to an undoped barrier. Both HEIWIPs and HIWIPs are grown by MBE, however, the larger space charge at the interface for HIWIPs will lead to effectively thicker interfaces, giving higher dark currents. For a QWIP structure the dark current is given by[8]

$$j_Q = e\frac{m_Q}{\pi\hbar^2\tau} k_B T \exp(-(\Delta - \alpha_Q E)/k_B T), \quad (2)$$

where m_Q is the carrier effective mass, τ is the time for a carrier to cross the well, and α_Q is the barrier lowering parameter for the QWIP. Since the activation energy is primarily determined by the desired λ_c for both detectors a comparison of the dark current effectively becomes a comparison of the pre-exponential factors. The small inhomogeneous broadening effect in QWIPs with bound-to-quasibound transitions would add a small reduction in the dark current which will be ignored. For detectors operating at 4.2 K and using a typical transit time of $\tau = 0.5$ ps and $\mu = 80\,{\rm cm}^2/{\rm V\,s}^{-1}$, $j_H/j_Q \sim 0.01$ for a p-type HEIWIP and an n-type QWIP for fields in the operating range and remains less than 1 up to room temperature. This gives larger currents than the HEIWIP for all temperatures in the operating range of the detector as long as $\alpha_H \leqslant \alpha_Q$. The fitting parameters will be the sum of parts corresponding to the sharpness of the interface (a common value α for QWIPs and HEIWIPs) and voltage drop between the center of the well/emitter and the interface. For the QWIP the field in the well is constant so the voltage drop is $ewE/2$ where w is the well thickness. For the HEIWIP/HIWIP structure, an effective thickness δ for the nonzero field region can be defined [see Fig. 2(b)] with the voltage drop $e\delta E$. Then the fitting parameters are $\alpha_Q = \alpha + ew/2$ and $\alpha_H = \alpha + e\delta$. The condition for HEIWIP dark current to be better than that for the QWIP is then $\delta < w/2$, a condition which should be satisfied under operating fields since charge will accumulate at the edges of the emitters in HEIWIPs. Thus the HEIWIP dark current is expected to be better than that for QWIPs due to increased capture/escape from the wells and a reduced barrier lowering effect. The dark current for a $\lambda_c = 28\,\mu$m QWIP was already larger than the dark current observed for the $\lambda_c = 65\,\mu$m HEIWIP detectors. At longer wavelengths absorption quantum efficiency strongly favors the HEIWIP structure over the QWIP concept. The free-carrier absorption coefficient α is $\sim N_D \lambda^N$ where N_D is the 3D doping density and $N \sim 2-3$ for wavelengths shorter than $\sim 8-12\,\mu$m (Ref. 6) and $N \sim 0$ for longer wavelengths.[3] For the QWIP the absorption coefficient is $\alpha \sim N_D^{\rm 2D}$ with the 2D doping density $N_D^{\rm 2D}$ being chosen to make the Fermi energy $2k_BT$ to achieve the best responsivity at $T_{\rm BLIP}$. Since $T_{\rm BLIP}$ will decrease as the desired wavelength range increases the absorption of QWIPs designed for long wavelengths will decrease. Thus both dark current and absorption favor the use of HEIWIPs over QWIPs for long wavelength detection.

The comparison of the first set of HEIWIP detectors to the current state-of-the-art Si:As, Si:Sb, and Ge:Ga detectors used in the far-infrared range is encouraging. For HEIWIPs photocurrent quantum efficiency was 24%, near the 25% obtained for Si BIB detectors to be used in the FORCAST camera for SOFIA.[9] The responsivity is also comparable to the values of 10–50 A/W for the stressed Ge:Ga detectors being developed for use in FIFI LS in SOFIA.[10]

This work was supported in part by the NSF under Grant No. ECS-98-09746 and by NASA under Grant No. NAG5-4950. The work at NRC was supported in part by Department of National Defense. The authors thank P. Chow-Chong and P. Marshall for device fabrication and S. J. Rolfe for SIMS measurements.

[1] E. E. Haller, M. R. Hueschen, and P. L. Richards, Appl. Phys. Lett. **34**, 495 (1979).
[2] I. C. Wu, J. W. Beeman, P. N. Luke, W. L. Hansen, and E. E. Haller, Appl. Phys. Lett. **58**, 1431 (1991).
[3] A. G. U. Perera, in *Handbook of Thin Film Devices Frontiers of Research, Technology and Applications*, Vol. 2 Semiconductor Optics, edited by M. H. Francombe, A. G. U. Perera and H. C. Liu (Academic, New York, 2000), pp. 135–169.
[4] A. G. U. Perera, H. X. Yuan, and M. H. Francombe, J. Appl. Phys. **77**, 915 (1995).
[5] A. G. U. Perera, S. G. Matsik, H. C. Liu, M. Gao, M. Buchanan, W. J. Schaff, and W. Yeo, Appl. Phys. Lett. **77**, 741 (2000).
[6] M. L. Huberman, A. Ksendzov, A. Larsson, R. Terhune, and J. Maserjian, Phys. Rev. B **44**, 1128 (1991).
[7] M. J. Kane, S. Millidge, M. T. Emeny, D. Lee, D. R. P. Guy, and C. R. Whitehouse, in *Intersubband Transitions in Quantum Wells*, edited by E. Rosenchenr, B. Vinter, and B. Levine (Plenum, New York, 1992).
[8] H. C. Liu, A. G. Steele, M. Buchanan, and Z. R. Wasilewski, J. Appl. Phys. **73**, 2029 (1993).
[9] L. D. Keller, T. L. Herter, G. J. Stacey, G. E. Gull, B. Pirger, J. Schoenwald, H. Bowman, and T. Nikola, Proc. SPIE **4014**, 86 (2000).
[10] D. Rosenthal, J. W. Bosman, N. Geis, L. Looney, A. Poglitsch, W. K. Park, W. Raab, and A. Urban, Proc. SPIE **4014**, 156 (2000).